

# Unwrapping highly wrapped phase using Nonlinear Multi Echo phase unwrapping

C. Fatnassi<sup>1,2</sup>, R. Boucenna<sup>2</sup> and H. Zaidi<sup>3</sup>

<sup>1</sup> Faculty of Biology and Medicine, University of Lausanne, Lausanne, Switzerland

<sup>2</sup> Radio-oncology Department, Hirslanden, Lausanne, Switzerland

<sup>3</sup> Department of Medicine and Molecular Imaging, Geneva University Hospital, Geneva, Switzerland

**Abstract**— The unwrapping problem has been a major topic of research for over a decade. A variety of algorithms were suggested, but a correct solution is by no means guaranteed. In addition, many of these techniques are time-consuming issues. In this work, we propose a simple and fast method, which combines conventional temporal unwrapping with a nonlinear phase model to unwrap highly wrapped Multi Echo data (Nonlinear Multi-Echo unwrapping). The approach was tested on simulated data and high-resolution *in vivo* brain data acquired from ten subjects at 3 Tesla demonstrating the promise of the proposed technique.

**Keywords**— Phase unwrapping, GRE, Temporal unwrap.

## I. INTRODUCTION

Susceptibility effects at high magnetic field is becoming an increasingly requested tool in many areas of MR imaging, which use the MR signal phase data, particularly in brain imaging. These include mapping local shift from the static magnetic field ( $\Delta B_0$ ) [1, 2], high-resolution phase imaging [3, 4], susceptibility weighted imaging (SWI) [5] and quantitative susceptibility mapping [6].  $\Delta B_0$  mapping characterizes the static magnetic field variations on the mesoscopic level [7], which can be associated with local concentrations of paramagnetic macromolecules that may reveal the physiology of disordered brain function [8]. It is applied for BOLD contrast studies [9] as well as for the assessment of iron content in the brain [10]. Because the range of phase values, which can be measured in MRI, is limited to  $2\pi$ , phase aliasing occurs, leading to discontinuities in specific regions (e.g. brain edges) of phase images which are known as “wraps.” Numerous pre-processing and post-processing methods with different degrees of success have been proposed to correct phase unwrapping. The existing unwrapping methods can be classified as either spatial or temporal approaches. Spatial methods use some regional characteristics of phase at a single echo time to identify wraps. Temporal methods are based on identifying wraps by means of the evolution of the phase in each voxel at two or more echo times [11]. However, spatial or temporal algo-

rithms fail if images are highly wrapped which may occur at long echo time acquisition ( $>20$ ms). In regions with high SNR and low susceptibility, such as the center of the brain, the mentioned algorithms remove the phase wraps, but in regions with low SNR and high susceptibility artefacts, e.g. near the paranasal sinus, most of the algorithms and especially temporal approaches fail or overcorrect the data most probably due to high phase wraps complexity and nonlinearity of the phase evolution. Regarding this issue, all temporal unwrapping methods assume that the phase evolves linearly as function of time. However in 2005, Zeng and Constable [12] demonstrated using simulation and *in vivo* data that the linear assumption is broken in the presence of a large field gradient, which is in agreement with what we have observed with 3T data, where the effect of susceptibility induced  $\Delta B_0$  is expected to be worse. To the best of our knowledge, there is a lack of a model that accounts for nonlinearity of phase evolution with time. We hypothesize that the over unwrapping observed is due to the linear phase evolution assumption being broken. Herein, we propose an analytical solution for nonlinear high wrapped phase unwrapping. This approach combines conventional temporal unwrapping and nonlinear phase model across echo time. We validated our hypothesis using simulation and *in vivo* data and compared it with 2D conventional Matlab unwrapping [13], 3D phase unwrapping [14] and two-dimensional phase unwrapping based on network programming [15].

## II. THEORY

The phase of the measured MR signal after an excitation at  $t_0$  and echo time TE can be described as:

$$\Phi(r, TE) = \Phi(r, t_0) + \gamma \Delta B_0 (TE - t_0) + \gamma \int_{t_0}^{TE} G_r(t) r dt \quad (1)$$

where  $\gamma$  the gyromagnetic constant and  $r$  is the spatial vector and  $G_r$  is the field gradient. Equation (1) can be expanded using the following Taylor series:

$$\Phi(r, TE) = \Phi(r, t_0) + \sum_{n=0}^{\infty} \frac{\gamma r^n}{n!} \int_{t_0}^{TE} G_r(t) (TE - t_0)^n dt \quad (2)$$

With  $r^n$  being the  $n^{\text{th}}$  derivative of time-dependent spin position. Under certain condition, equation (2) can be approximated by:

$$\Phi(r, TE) = \Phi(r, t_0) + \gamma r^0 \int_{t_0}^{TE} G_r(t) dt + \gamma v \int_{t_0}^{TE} G_r(t) t dt + \dots \quad (3)$$

where  $v$  represents the phase velocity, which can be calculated as follows:

$$v(r) = \frac{\Phi(r, TE)}{\gamma \int_{t_0}^{TE} G_r(t) t dt} = \frac{\Phi(r, TE)}{\pi VENC} \quad \text{and} \quad VENC = \frac{\pi}{\gamma \int_{t_0}^{TE} G_r(t) t dt} \quad (4)$$

VENC is the velocity encoding which is computed in order to know where the phase wraps will occur. No wraps occur if the selected echo time  $TE < VENC$ . As such,  $\Delta TE$  can be selected on the basis of knowledge of the typical range of  $\Delta B_0$  values encountered at the field strength in question to avoid unintentional phase wrapping. The nonlinearity of the phase evolution as function of echo time was observed and demonstrated [12,16] (Fig. 1). In the presence of large susceptibility artefacts, the linear assumption of the phase evolution is broken. To overcome this problem, we propose a model to account for this nonlinearity using a 1D random walk theory when the images are acquired at long TE ( $>20\text{ms}$ ). The phase of the  $n^{\text{th}}$  voxel can be described by:

$$\varphi_n(TE_n) - \varphi_n(TE_1) = \varepsilon_n(TE_n) = (N \cdot \beta_n)^{\frac{1}{2}} \delta\varphi_n(\Delta TE) \quad (5)$$

where  $n$  is the echo number,  $\varepsilon_n$  is the nonlinear phase jump and  $\beta_n$  is a coefficient which can be calculated using the random walk theory [16]. Finally, we combine the nonlinear approach to describe the temporal phase evolution and the conventional temporal phase unwrapping to correct from high phase aliasing. The phase wraps that occur at certain TE can be removed by substituting the wrapped phase value using the following analytical expression:

$$\varphi_{n,unwrap}(TE_n) = \frac{1}{N} \left[ \sum_n \left[ (\varphi_{n-1,wr} - 2\pi INT \left( \frac{\varphi_{n-1,wr} - \varphi_{n,wr}}{2\pi} \right) - \Delta B_0 \sum_N TE) \right] \right] + (N \cdot \beta_n)^{\frac{1}{2}} \delta\varphi_n(\Delta TE) \quad (6)$$

where  $INT$  denotes the operator integer and  $\delta\varphi$  is the phase jump computed from the phase data [16].

### III. MATERIALS AND METHODS

To assess the accuracy of our approach in the presence of high phase wraps at long echo time; we used simulated wrapped phase with different wraps complexity (Fig. 2) and different noise levels. The percentage accuracy was calculated as the mean over all image voxels as  $100 \times (1 - |(\varphi_{unwrap} - \varphi_{unwrap}) / \varphi_{unwrap}|)$ . Ten *in vivo* scans were performed on a 3T Magnetom Trio (Siemens Healthcare, Erlangen, Germany) using 32-channel phased-array coil. Data were acquired using a 3D bi-polar multi gradient echo sequence. Our approach need a minimum of 2 acquisitions at different echo times: the first echo is selected to be smaller than VENC. The second echo is acquired with long TE ( $>20\text{ms}$ ). Acquisition parameters for the tow echoes were: TR/TE1 /TE2 = 47/1.23/30.75ms, flip angle  $8^\circ$ , 1.6 mm<sup>3</sup> isotropic resolution and a matrix size of  $136 \times 136 \times 112$ , Grappa parallel imaging with acceleration factor of 2, and phase partial Fourier sampling factor of 6/8. Our method was compared with 2D conventional unwrapping, 3D phase unwrapping and 2D phase-unwrapping algorithms based on network programming.

### IV. RESULTS AND DISCUSSION

Fig. 1 shows the phase behaviour in presence of large field gradient ( $>40\text{Hz/cm}$ ). The phase evolution appears nonlinear and consequently, unwrapping the phase with a simple temporal approach that relies on linear approximation may lead to phase over estimation.

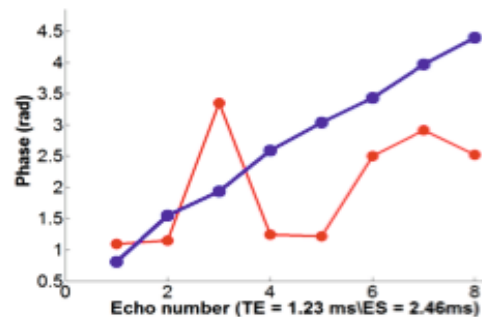


Fig 1. Phase evolution as function of time in the presence of low (blue) and high (red) field gradient

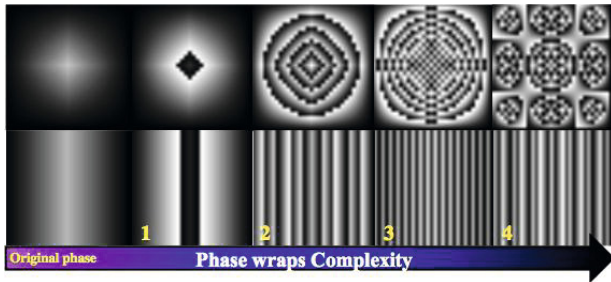


Fig 2. Example of phase wraps with increasing topography complexity on simulated data

Fig. 2 illustrates the increased complexity of the simulated data. Fig. 3 (top) shows the accuracy of the four unwrapping methods as function of wraps complexity. It can be seen that our NME method performs better by maintaining an accuracy of 100% even for high and complex phase wraps. The accuracy of the spatial unwrapping-based methods reduced sharply when the complex topographies of the wraps increase (at level 3). In Fig. 3 (bottom), the accuracy of the four methods is plotted against the noise level added to the phase data. Only NME and Costantini approaches demonstrate a good robustness and insensitivity in unwrapping the phase in the presence of high noise level.

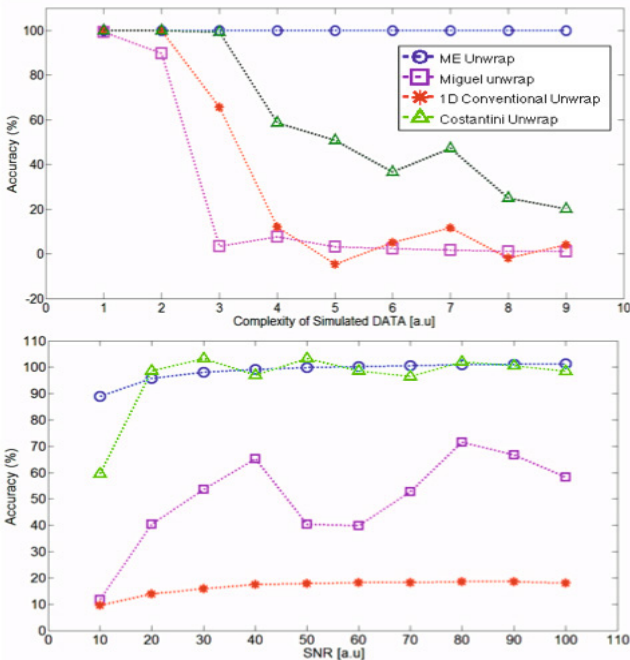


Fig 3. Accuracy of the 4 unwrapping methods as function of wraps complexity (top) and noise level (bottom).

Fig. 4 illustrates the results achieved by the 4 methods

using simulated data. One can notice that spatial 2D, 3D and conventional Matlab unwrapping methods fail when the topography of the phase wraps increase (>3). Nevertheless, NME successfully removes all phase aliasing even for high wraps complexity.

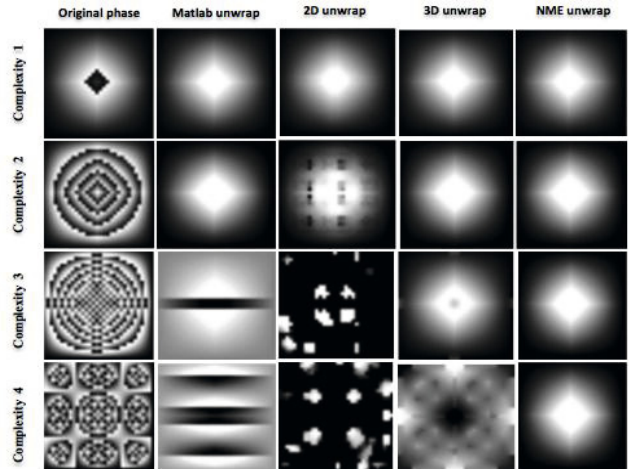


Fig 4. Example of results achieved on simulated data.

Fig. 5 demonstrates the accuracy of the three methods in unwrapping phase acquired with long echo time (TE = 30.75ms). The phase wraps occur near the brain edges and in the paranasal sinus where the field gradient is large (see arrows). The spatial unwrapping methods tend to smooth the data to simplify the spatial wraps complexity but lead to some spatial information loss. In addition, these approaches fail in regions with high wraps. The NME method successfully addresses phase unwrapping even in regions with high wraps. In Fig. 6, we compare NME using a conventional temporal phase unwrapping. Both methods provide good results. Although, conventional temporal unwrapping fails to unwrap phase in regions with high wraps and especially where the phase evolution is no longer linear as a function of echo time (see arrows). The NME method overcomes this problem and provides a homogeneous phase map.

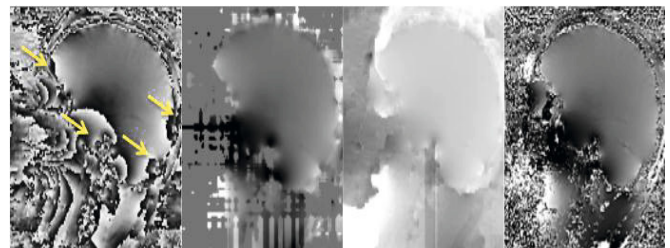


Fig 5. From left to right: original phase, 2D unwrap, 3D unwrap and NME unwrap.

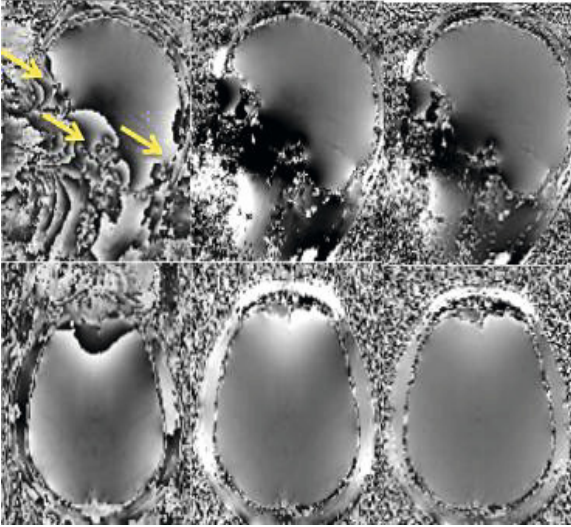


Fig 5. From top to bottom: sagittal and axial phase slice. From left to right: original phase, conventional temporal unwrap and NME unwrap.

## V. CONCLUSION

The NME method allows phase images to be unwrapped even if the phase evolution between echo times is much greater than  $\pi$ . This approach overcomes the phase nonlinearity problem at very long echo time. The proposed method needs only two echoes and additional echoes may enhance the unwrapping in the presence of noise. The speed and simplicity of the approach makes it ideally suited for wide use in the field of MR phase unwrapping.

## REFERENCES

1. Jezzard P et al. (1995) Correction for geometric distortion in echo planar images from B0 field variations. *Magn Reson Med* 34:65–73.
2. Robinson S et al. (2011) B0 mapping with multi-channel RF coils at high field. *Magn Reson Med* 66:976–988.
3. Rauscher A et al. (2005) Magnetic susceptibility weighted MR phase imaging of the human brain. *AJNR Am J Neuroradiol* 26:736–742.
4. Duyn J et al. (2007) High field MRI of brain cortical substructure based on signal phase. *Proc Natl Acad Sci USA* 104:11796–11801.
5. Reichenbach J et al. (1997). Small vessels in the human brain: MR venography with deoxyhemoglobin as an intrinsic contrast agent. *Radiology* 204:272–277.
6. Reichenbach J et al. (1998) High resolution venography of the brain using magnetic resonance imaging. *MAGMA* 6:62–69.

7. Dimitriy A et al. (2012) Voxel Spread function Method for correction of magnetic field inhomogeneity Effects in Quantitative Gradient Echo based MRI. *Magn Reson Med* 70:1283–1292.
8. An H et al. (2003) Impact of intravascular signal on quantitative measures of cerebral oxygen extraction and blood volume under normo and hypercapnic conditions using an asymmetric spin echo approach. *Magn Reson Med* 50:708-716.
9. Gandon Y et al. (1994) Hemochromatosis: Diagnosis and quantification of liver iron with gradient-echo MR imaging. *Radiology* 193:533-538.
10. Frahm J et al. (1988) Direct Flash MR imaging of magnetic field inhomogeneities by gradient compensation. *Magn Reson Med* 6:474-480.
11. Robinson S et al. (2014) A Method for Unwrapping Highly Wrapped Multi-echo Phase Images at Very High Field: UMPIRE. *Magn Reson Med* 72:80-92.
12. Huairan Zeng et al. (2002) Image distortion Correction in EPI: Comparison of Field mapping with Point Spread Function mapping. *Magn Reson Med* 48:137-146.
13. Phase unwrap. Mathworks USA at <http://ch.mathworks.com/help/matlab/ref/unwrap.html>.
14. R. Cusack et al. (2002) New Robust 3-D Phase Unwrapping Algorithms: Application to Magnetic Field Mapping and Undistorting Echoplanar Images. *NeuroImage* 16: 754-764.
15. Costantini et al. (1998) A novel phase unwrapping method based on network programming. *IEEE Transactions on Geoscience and Remote Sensing* 36:813-821.
16. C. Fatnassi et al. (2013) European Society of Magnetic Resonance in medicine and Biology. 26:234:235.

Author: C. Fatnassi  
 Institute: radio-oncology department, Clinique Bois-Cerf  
 Street: Avenue d'Ouchy, 31  
 City: Lausanne  
 Country: Switzerland